Characterizing urban heat islands in karst areas-the case of Kunming and Guiyang in Southwest China

Ruixue Fan[1,2]*, Yangyang Wu[1,2]*, Qiwei Chen[1,2], Youjin Wang[1], Lianjin Li[1], Dongyu Shi[1], Rong Xu[1], Yuting Xia[1] and Yuting Cheng[1]

[1]School of Geography and Resources, Guizhou Education University, Guiyang, China, [2]Guizhou Provincial Key Laboratory of Geographic State Monitoring of Watershed, Guizhou Education University, Guiyang, China

Urban heat island (UHI) has posed a threat to sustainable development, and the identification of the spatial characteristics of UHI is a prerequisite for the mitigation of UHI effects. Taking Kunming City and Guiyang City in the karst region of Southwest China as two examples, this study utilized spatial econometric modeling and random forest regression to identify and compare the spatial distribution and impact of urban heat islands related to topographic and urban morphology. The results indicated that the UHI in Kunming and Guiyang mainly monocentrically and polycentrically distributed, respectively, and the urban heat island intensity (UHII) in Kunming was significantly higher than that in Guiyang. The spatial error model effectively reflected the influence of topography and urban form on UHII, and the random forest regression model objectively measured the contribution of different influencing factors to UHII. Enhanced vegetation index (EVI), population density (PD), percentage of impervious surface (PIS), ground sky view factor (GSVF), building density (BD) and percentage of water bodies (PW) had similar effects and contributions to the UHII in the two cities, while urban surface roughness (USR) contributed less than topographic slope (SLOPE) on UHII in Kunming, and the SLOPE contributed less than USR in Guiyang. In the karst ecologically fragile zone, the morphology of Kunming and Guiyang are mainly shaped by the topography, which can be characterized as monocentric and polycentric, respectively. And the UHI distribution and UHII were also closely related to topographic patterns. EVI, SLOPE and PW, all showed inhibitory effects on UHII, and EVI contributed the most. PD, PIS, USR and BD, exacerbate the UHII, with PD contributing the most. The above conclusions can provide a reference for policymakers and urban planners to optimize urban morphology and mitigate urban heat island.

KEYWORDS

topography, urban morphology, urban heat island, spatial econometric modeling, random forest regression modeling

1 Introduction

Urban heat island (UHI) is a phenomenon that the atmospheric and surface temperatures in urban areas are significantly higher than that in nearby rural areas due to changes in urban structure, land cover, heat release by human activities, and geoclimatic factors (Howard, 1818; Voogt and Oke, 2003), which not only leads to localized climate and

phenology malfunctions (Kotharkar and Surawar, 2018; Kabano et al., 2021), increases the consumption of energy for cooling (Li et al., 2019), but also allows the accumulation of hazardous compounds, and even affects the health of the inhabitants (Patz et al., 2005; Bobb et al., 2014). The acceleration of urbanization process intensifies human activities, leading to the destruction of natural ecosystems, the reduction of vegetation cover, and the intensification of soil erosion. UHI effect has become the focus of global sustainable development. The development of strategies to mitigate UHI obliges the studies of the spatial-temporal processes and the drivers of UHI to provide theoretical guidance (Fahmy and Sharples, 2009; Aboelata, 2020).

Present studies have shown that the factors affecting the spatial and temporal distribution and urban heat island intensity (UHII) are mainly urban morphology (Fang et al., 2015; Zhou et al., 2017; Zhou and Chen, 2018), land use type/land cover (Coseo and Larsen, 2014; Bokaie et al., 2016; Deilami et al., 2018), climatic background (Zhao et al., 2014; Sun et al., 2019a), and anthropogenic heat release (Jauregui, 1997; Doan, Kusaka, and Nguyen, 2019). Topography, as a natural form, directly contributes to the characteristics of urban morphology, thus highly relates to the urban heat island (Mirzaei, 2015; Equere et al., 2021). Generally, under the influence of the flat topography, it is naturally to form a monocentric urban structure with a concentrated core and dispersed periphery, while hilly areas tend to show a polycentric urban structure with overall dispersion and site-specific concentration affected by the fluctuation of topography (Peng et al., 2015; Liu et al., 2022). Monocentric cities gather a large number of buildings and populations, and the long-distance commuting of people leads to high-density heat emission of human activities, which has an obvious effect on the enhancement of UHI (Chun and Guldmann, 2014; Manoli et al., 2019; Liu et al., 2021b). The polycentric city structure has a significant effect on the reduction of UHI (Zhou et al., 2011; Lin et al., 2013; Zhang et al., 2017), and it is considered to be the optimal urban form for mitigating UHI (Liu et al., 2021a). However, some researchers proposed a different point of view, which is that the polycentric structure may cause employment dispersion, work-housing imbalance, exacerbate urban traffic congestion, energy consumption, and anthropogenic heat release (Lin et al., 2015; Sun et al., 2019b; Yue et al., 2019), and lead to the spread of UHI to the subcenters, which will affect the thermal environment of the city (Stone and Rodgers, 2001; Liang et al., 2020). In addition, the layout, density, shape, and orientation of buildings within the city (Grosso, 1998), their overall size, contour, and mono/multicentricity jointly affect the spatial pattern of the urban climate (Zhou et al., 2017; Guo et al., 2020), and therefore, the landscape pattern (Estoque et al., 2017; Li et al., 2017), building morphology (Yan et al., 2023; Mo et al., 2024), and ground sky view factor (GSVF) (Mo et al., 2024) have a significant impact on the urban heat island intensity (Equere et al., 2021) etc. All contribute to urban heat island intensity.

Karst areas have the most typical fragile environment and complex human-land ecosystems, so the challenge of heat island effect caused by urbanization is much greater than that of other cities in non-karst areas, which calls for investigations of UHI effects in karst landscapes. Karst landscapes are widely distributed in southwest China (Zhang et al., 2022). With the accelerating urbanization process, UHI effect in karst ecologically fragile areas become an issue that must be faced for sustainable development. Some studies have found that a large

number of Abnormal heat islands (AHI) exist in karst areas (Deng et al., 2018; Liao et al., 2022), and the intensity of AHI increases in almost all directions with urban expansion. The random sprawls of urban area not only intensify the urban heat island in the built-up area, but also induce the increase of AHI intensity (Liao et al., 2022). However, there was no in-depth study of its characteristics and factors, which is important to mitigate UHI in karst regions.

Urban green space is one of the important components of urban ecosystem and plays an important role in alleviating urban heat island effect (Semenzato and Bortolini, 2023). Affected by karst geomorphology, isolated peaks and peaks cluster are distributed in karst cities. The urban green space system is mainly mountain green space, which is a long-formed residual natural ecosystem with the vertical vegetation distributed. Therefore, the effect of urban green space on urban thermal environment in karst area is different from that in non-karst cities. However, the existing research on karst urban thermal environment mainly focuses on the spatio-temporal variation of urban heat island and the mitigation effect of mountain green space on urban heat island (Karunaratne et al., 2022; Chen et al., 2021). There is little analysis of the influence of urban heat island in karst area considering multiple factors comprehensively.

To fill the gaps, we aimed to identify the UHI distribution and the corresponding comprehensive influencing factors in Karst regions. We analyzed the potential influences of landforms and urban forms on UHI of Kunming City and Guiyang City in the Southwest China. We selected variables combined with the terrain and urban morphology such as building density (BD) (Perini and Magliocco, 2014), slope of topography (SLOPE) (Guo et al., 2020), population density (PD) (Ramírez and Léa Cristina, 2019), ground surface sky view factor (GSVF) (Liu et al., 2022), urban surface roughness (USR) (Lu et al., 2021), percentage of impervious surface (PIS) (Lu et al., 2021), and enhanced Vegetation Index (EVI) (Sun et al., 2021), and percentage of water (PW) (Wang et al., 2015) and explored their influences based on the spatial econometric model. Furthemore, random forest regression model was introduced, which revealed the distribution of the UHI in the karst ecologically fragile zone, and provided a basis not only for optimizing the urban structure of the karst region to mitigate the urban heat island, but also for decision-making to promote sustainable development. Because of the large scale and wide range view of satellite products, many scholars have paied attention to the surface UHI in recent decades (Peng et al., 2012; Zhou et al., 2014; Zhou et al., 2018). We dealed with the surface temperature in this study.

2 Study area and data sources

2.1 Research area

Kunming City and Guiyang City are the capital cities of Yunnan Province and Guizhou Province, respectively, and are also important political, economic and cultural centers for regional development in southwest China. As China's open door to Southeast Asia, Kunming City located at the north-south international corridor, and the center of urban areas includes Wuhua District, Panlong District, Guandu District, Xishan District, Chenggong District. Guiyang City is featured as an industrial base, business and tourism center, an important transportation and communication node in southwest
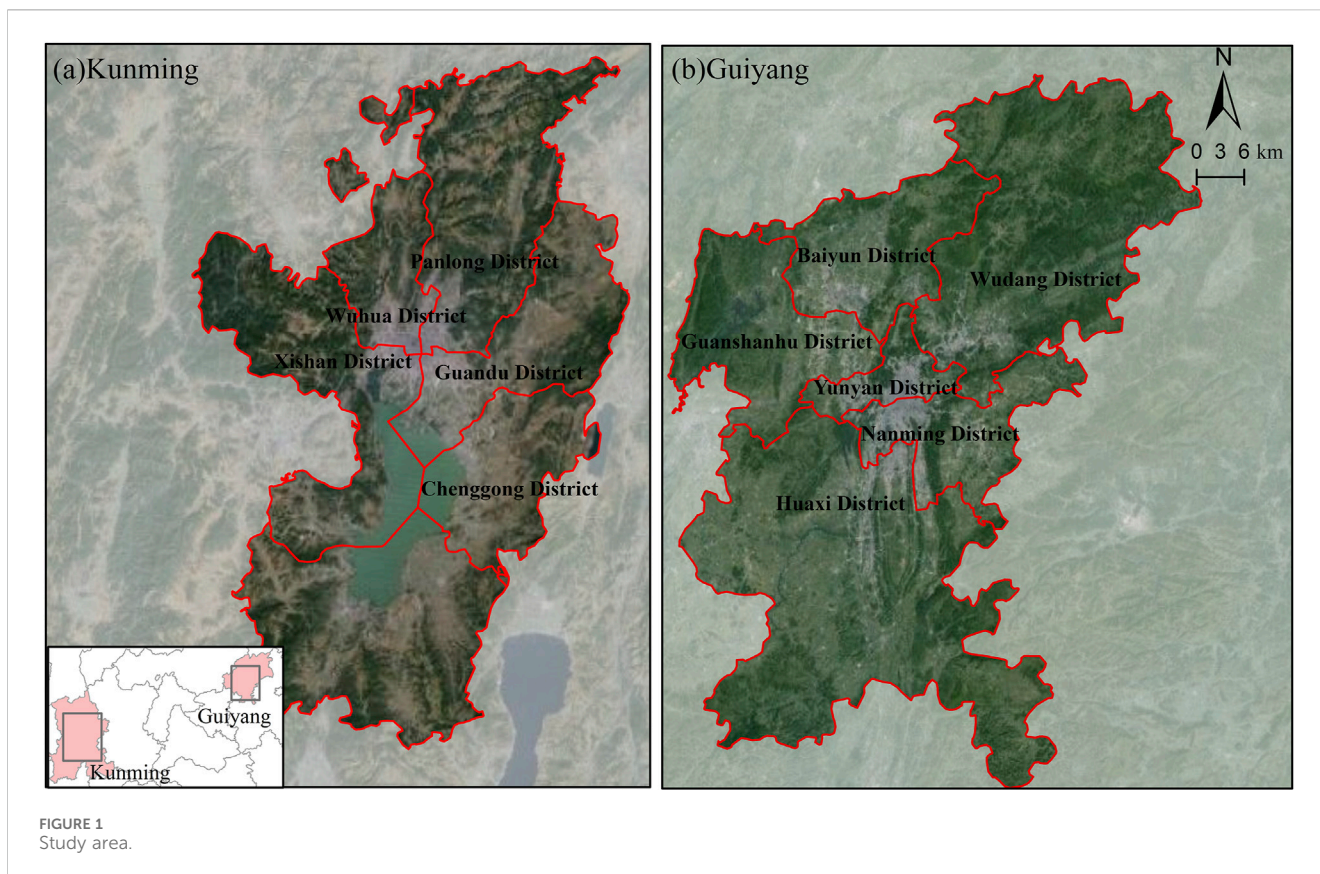
FIGURE 1
Study area.

China, and its central urban area includes Yunyan District, Nanming District, Baiyun District, Wudang District, Guanshanhu District and Huaxi District (Figure 1).

Kunming is located in the middle of Yunnan-Guizhou Plateau (102°10′~103°40′E, 24°23′~26°22′N), whose urban area is situated on the Northern Dianchi Basin and surrounded by mountains on the west, north and east sides. With a flat topography about 763 km², Kunming has formed a typical single-center city structure with Wuhua District as the main core in a radial or concentric-circle development pattern. Guiyang city is located in the eastern end of Yunnan-Guizhou Plateau (106°07′~107°17′E, 26°11′~26°55′N), sporadically distributed in small and narrow areas separated by the Baihua Mountain, Qianling Mountain, and Nanyue Mountain. By the limitation of dispersed topography, Guiyang is a multi-center urban form.

Both Kunming and Guiyang situate on the Yunnan-Guizhou Plateau, with similar latitude, longitude and altitude, dominated by subtropical evergreen broad-leaved vegetation. Both of them are located at karst region in Southwest China. With the acceleration of urbanization, the UHI effect is significantly enhanced in Kunming and Guiyang. Therefore, we selected Kunming City and Guiyang City (Figure 1) for a comparative study.

2.2 Data sources

We used urban vector boundary data, Landsat 8 Level 2 remote sensing data (30 × 30), built-up area data, building contours and heights data, road data, DEM data, impervious surface data, and population density data of Kunming City and Guiyang City. The enhanced Vegetation index (EVI) product of satellite remote sensing data inversion is one of the ecological environment data products launched by the geographic remote sensing ecological network platform (http://www.gisrs.cn/infofordata?id=071e471f-f6e6-400e-9986-75f91a9c1894). The product has been verified by the expert group and is of good quality. Specific data sources are shown in Table 1.

The built-up area data and road vector data of Kunming City and Guiyang City in 2020 were obtained from Scientific Data Bank (https://www.scidb.cn/) and OpenStreetMap (https://www.openstreetmap.org/). We used road vector data to divide built-up districts into block areas in order to analyze the relationship between surface temperature and independent variables. We extracted 34,518 and 20,155 blocks in the built-up areas of Kunming City and Guiyang City (Figure 2).

3 Materials and methods

3.1 UHI intensity calculation

The temperature units of Landsat 8 Collection 2 Level 2 Surface Temperature used in this study is in Kelvin, which we converted to Celsius (Equation 1). The UHII is expressed as the temperature difference between the temperature of each image and the average the mean of *LST*, which calculated by Equation 2.

$$LST = B_{10} - 273.15 \qquad (1)$$

where *LST* is the pixel surface temperature and B_{10} is the Landsat 8 Collection 2 Level 2 ST product.

TABLE 1 Data and sources.

Data	Source
Urban vector boundary	China temporal sequence administrative map
Landsat 8 Level 2	USGS (https://earthexplorer.usgs.gov/)
Built-up area	ScienceDB (https://www.scidb.cn/)
Building contours and heights	ScienceDB (https://www.scidb.cn/)
Road	Openstreetmap https://www.openstreetmap.org/
DEM	DAAC https://nasadaacs.eos.nasa.gov/
Impervious surface	https://www.x-mol.com/groups/li_xuecao/dongtaizhitu
Population density	The 7th National census data
EVI	http://www.gisrs.cn/infofordata?id=071e471f-f6e6-400e-9986-75f91a9c1894

TABLE 2 Description and sources of independent variables.

Categories of variables	Variables	Abbr	Description	Calculation	Data source
Topography factors	Topographic slope	SLOPE	The ratio of vertical height and horizontal distance of the slope	$SLOPE = \arctan(\frac{H\max - H\min}{L}) \times \frac{180}{\pi}$, where H_{max} and H_{min} are the highest and lowest elevations of the block, respectively, and L is the distance between them	DEM
	Ground sky view factor	GSVF	The ratio between the radiation received by a planar surface and the entire hemispheric radiating environment	$GSVF = 1 - \sum_{n=1}^{n} \sin^2 \beta_i (\alpha_i/360°)$, where n is the total number of the angle elements of the obstacles in the hemispheric environment, and α_i and β_i reflect the elevation and azimuth angles of the angle element i, respectively	DEM and 3D building models
	Urban surface roughness	USR	The relative height difference of urban surface in block	$USR = (H_{max} - H_{min}) \times (1 - A_p/A_B)$, where H_{max} 和 H_{min} are the highest and lowest elevations of the block, respectively, A_P and A_B are the flat area and total land area of the block, respectively	DEM and 3D building models
Urban form factors	Building density (%)	BD	The ratio of building base area to block area	$BD = \sum_{i=1}^{n} A_{bi}/A_B$, where A_{bi} is the base area of building i, n is the number of buildings in a block, and A_B is the area of the block	3D building models
	Population density	PD	The average population density of the block	$PD = \sum_{i=1}^{n} A_{pi}/A_B$, where A_{pi} is number of people in the block. A_B is the area of the block	The 7th National Census Data
Land use/cover factors	Percentage of impervious surface (%)	PIS	The ratio of impervious surface area to block area	$PIS = A_{isi}/A_B$, where A_{isi} is the area of impervious surfaces such as roads, roofs, and other paved surfaces, and A_B is the block area	Landsat derived data
	Enhanced vegetation index	EVI	The mean enhanced vegetation index in block	$EVI = 2.5 \times (NIR - Red)/NIR + 6.0 \times Red - 7.5 \times Blue + 1)$, where NIR/Red/Blud are atmospherically-corrected surface reflectance of Landsat image bands	Landsat derived data
	Percentage of water (%)	PW	The ratio of water bodies in block area	$PW = \sum_{i=1}^{n} A_{wi}/A_B$, where A_{wi} is the area of water body i, n is the number of water bodies in a block, and A_B is the area of the block	Land use maps

$$UHII = \frac{T_s - T_m}{SD} \qquad (2)$$

where T_S is the LST of the pixel, T_m is the mean of LST, SD is the standard deviation of LST.

3.2 Variables selection and acquisition

In the early study of urban heat island, the topographic effect was seldom considered (Peng et al., 2012; Rizwan et al., 2008; Zhou et al., 2014). With the acceleration of urbanization in China, Li et al. (2017), Guo et al. (2020), Liao et al. (2022) noted the rapid expansion of mountain cities and their urban heat island problems. Existing research shows that topography plays an important role in the formation and intensity of urban heat island. Especially on the undulating ground, topographic factors have a strong influence on the intensity of urban heat island (Equere et al., 2021; Mirzaei, 2015; Zhou et al., 2014). In karst areas, the surface fluctuation is more obvious. Therefore, topographic factors are important factors in the study of urban heat island intensity in karst areas.
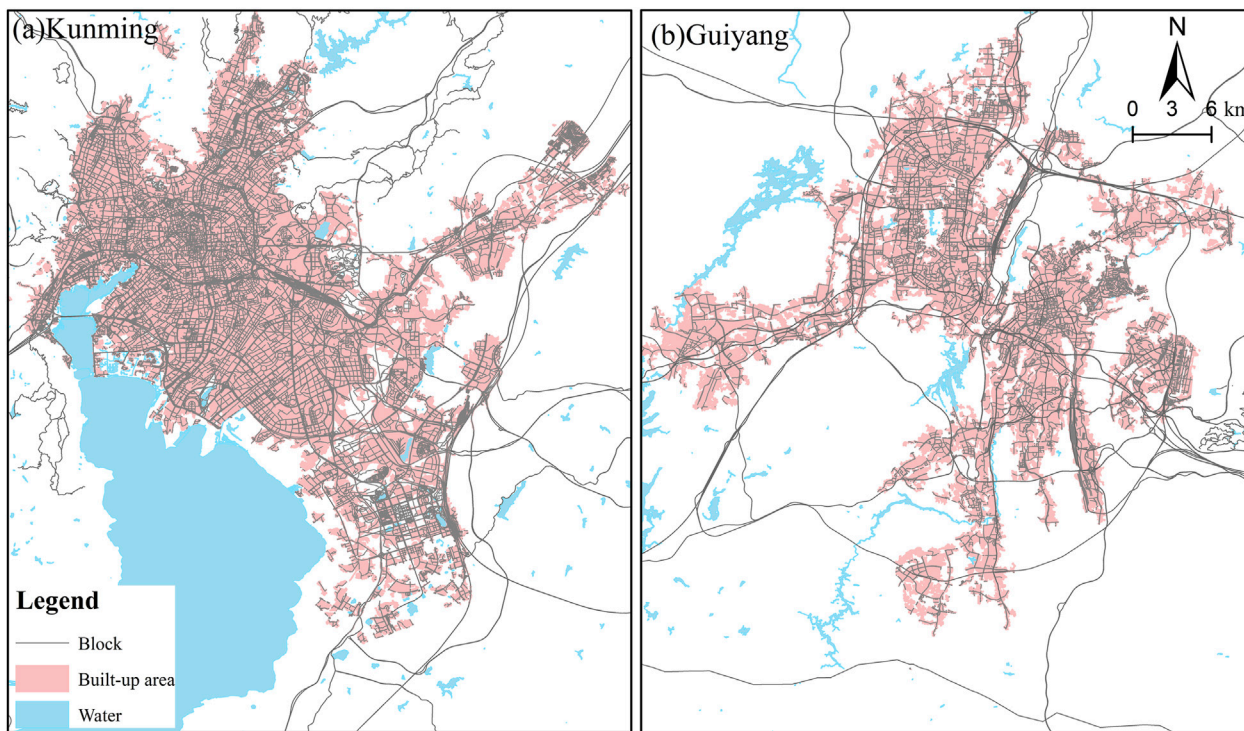
FIGURE 2
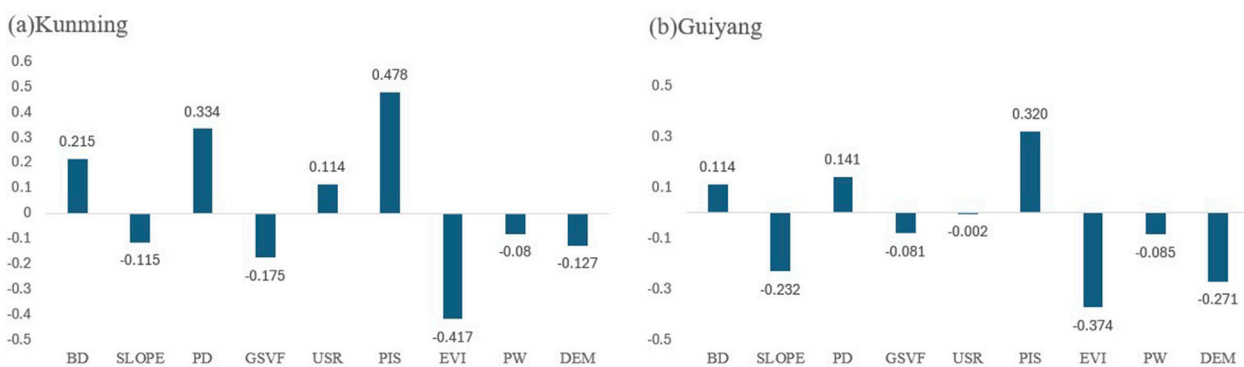Block map of urban built-up area.

FIGURE 3
Relative contribution of multiple factors to UHII.

Urbanization is the product of human activities. Therefore, population distribution and human activities are important factors affecting urban heat island, such as population density and spatial distribution of building groups (Cui et al., 2017; Kotharkar and Surawar, 2016; Peng et al., 2012; Yue et al., 2019). Land resources are limited in karst areas, so population density and building groups are important factors affecting urban heat island. Description and sources of selected variables were showed as Table 2. Their statistics were described in Table 3.

Heat island is comprehensively affected by the topographic fluctuation, underlying surface properties, slope orientation, meteorological conditions, different seasons and diurnal changes.

Factors for this study were selected by the degree of correlation between factors and the ground temperature (Figure 3). DEM and SLOPE are correlated factors because the latter is directly calculated from the former, they show a similar degree of correlation to UHII, while the DEM generally highly correlated to the other factors than SLOPE. Although the temperature of the atmosphere decreases with increasing altitude, considering the small relative elevation difference (200–300 m) and the DEM's higher correlation to the other factors, SLOPE was selected as the factor for the analysis.

According to the previous studies on the factors affecting urban heat island and the characteristics of karst areas, we choose topographic factors, urban form factors and land use/cover
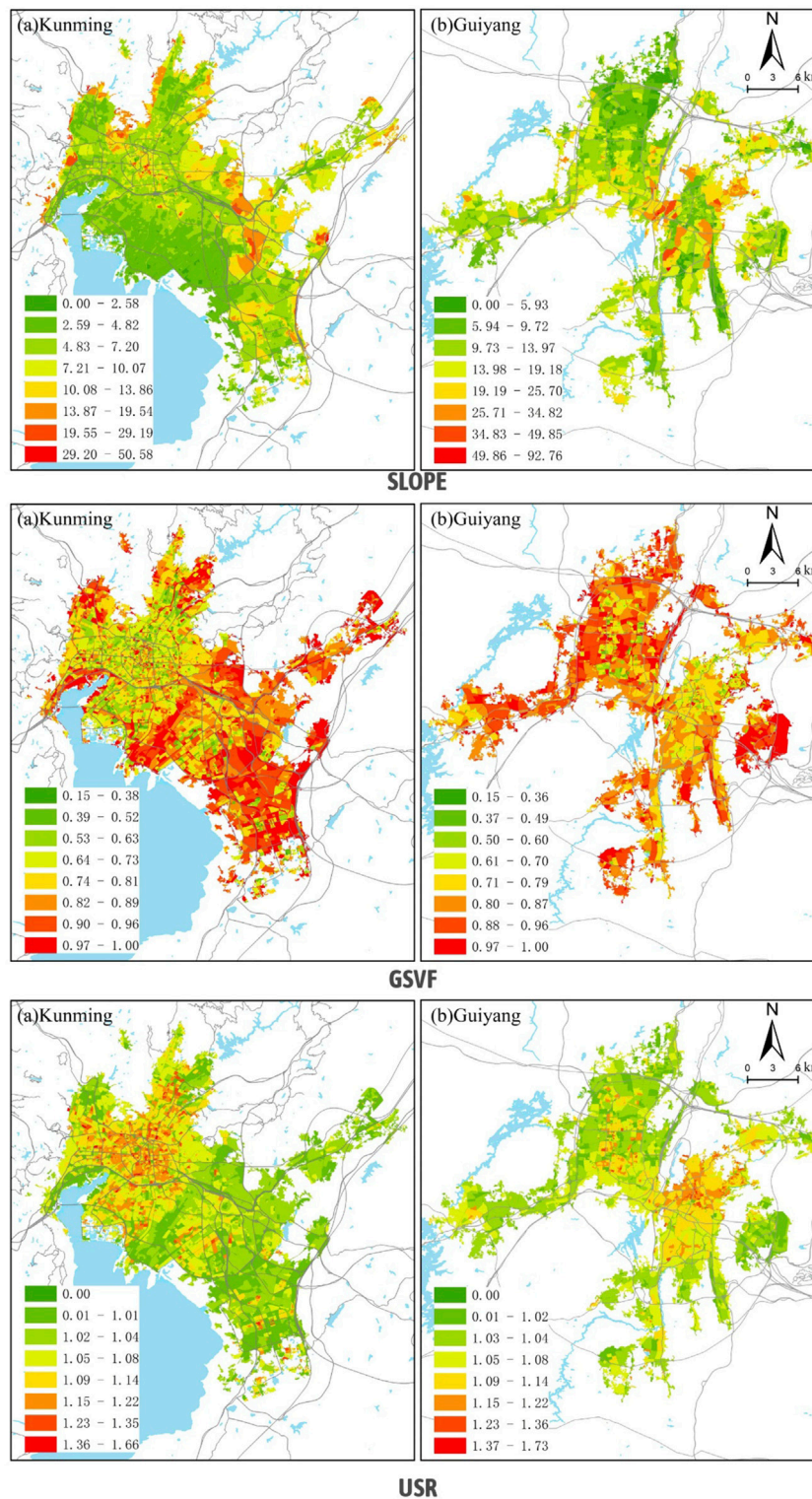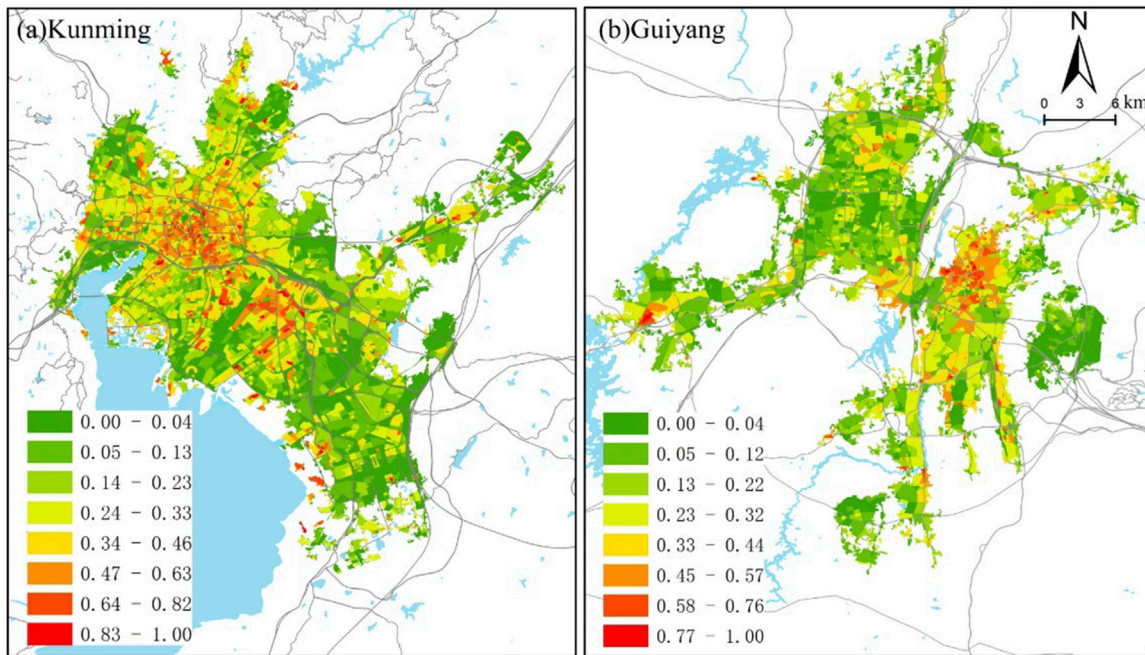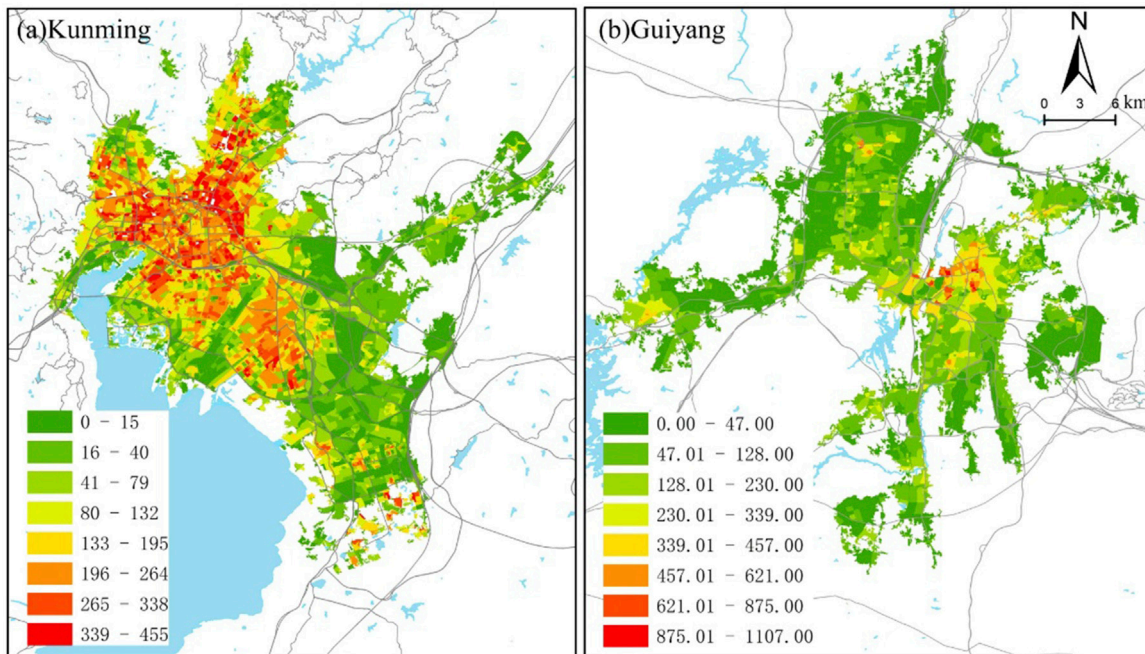
FIGURE 4
Spatial distribution of topography factors.

factors to carry out research. For topography factors, we selected SLOPE, GSVF and USR (Figure 4). SLOPE is the steepness of a surface unit that warms the air by altering the thermal properties of the urban subsurface (Guo et al., 2020). GSVF, is a comprehensive indicator for assessing the impact of building height and density on the urban heat island effect (Perini and Magliocco, 2014; Liu et al., 2022). USR is important for understanding aspects of urban climate and thermal environment, and significant correlation exists between rough undulating surface of topographic factors and UHI intensity (Lu et al., 2021). For urban form factors, we selected BD and PD

FIGURE 5
Spatial distribution of urban form factors.

(Figure 5). BD, as one of the key indicators of urban building form, is the most common urban form factor in previous studies. PD is the number of people per unit of land area, which reflects the degree of aggregation and dispersion of the population, and affects the intensity of UHI by emitting heat (Ramírez-Aguilar, Souza,

2019). For land use/cover factors, we calculated PIS, EVI and PW (Figure 6). PIS, as a core parameter for assessing the influence of urban surface characteristics on the heat island effect, has a positive correlation with urban heat island intensity (Lu et al., 2021). EVI is an indicator used to monitor vegetation

FIGURE 6
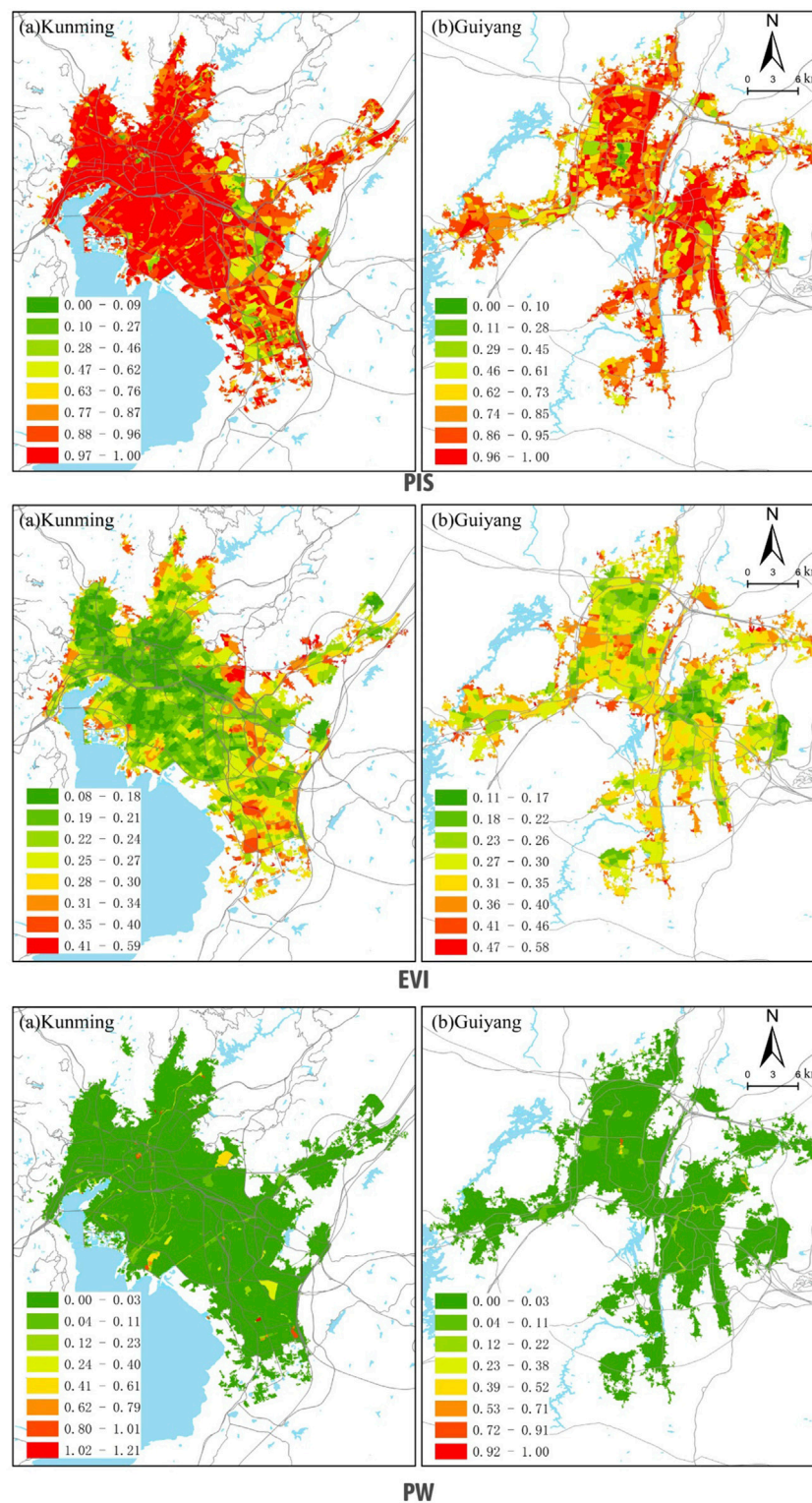Spatial distribution of land use/cover factors.

growth and cover, which can reflect the impact of climate on vegetation and thus help predict ecosystem response to climate change (Sun et al., 2021). PW plays an important role for the

mitigating surface temperature and urban heat island effect, and the width of the water body also affects its ability to mitigate the heat island effect (Wang et al., 2015).

3.3 Methods

We used multiple linear regression (MLR) models (Equation 3), and spatial econometric models (Equations 4, 5) to analyze the effects of topography factors and urban form on UHI intensity. Multiple linear regression captures the existence of a linear relationship between the independent and dependent variables. Meanwhile, considering that temperature varies non-stationary in space, we use the spatial error model (SEM) and spatial lag model (SDM) in spatial measurement model to explore the non-stationary relationship between the independent variables and the dependent variable, thus compensating for the shortcomings of multivariate linear regression model (MLR). Due to the local nonlinear correlation and threshold effect of each influencing factor on UHI, the linear positive or negative correlation alone is not enough to accurately reveal its driving role. Therefore, a random forest (RF) regression model was introduced to calculate the contribution of the independent variables to the dependent variable. We used Python code in Spyder 5.4.3 to excute RF model, and we set the number of trees to 200.

The traditional multivariate linear model can be expressed as:

$$UHII = \alpha + \beta X + \varepsilon \qquad (3)$$

where $UHII$ is the UHI intensity of the blocks of Kunming and Guiyang, α is a constant, β is a regression coefficient, and ε is a random error.

The spatial error model can be expressed as:

$$UHII = \rho W_{UHI} + \rho X + \varepsilon, \varepsilon \sim \left(0, \delta^2 \ln\right) \qquad (4)$$

where $UHII$ is the dependent variable, ρ is the spatial lag factor, W_{UHI} is the spatial weight matrix, X is the independent variable matrix, β is the coefficient vector, and ε is the random error.

The spatial lag model can be expressed as:

$$UHII = \beta X + \lambda W_\mu + \varepsilon, \varepsilon \sim \left(0, \delta^2 \ln\right) \qquad (5)$$

where λ is the spatial error factor, W_μ is the spatial weight matrix, and δ is the random error.

4 Results and analysis

4.1 UHI intensity

The results of UHI intensity spatial distribution (Figure 7) showed that there are obvious differences in the spatial distribution patterns between Kunming and Guiyang. First, the distribution of UHII in Kunming is significantly higher than that in Guiyang, which may be inextricably related to the process of urbanization and urban morphology. Second, the high-intensity area of UHI distributed in Kunming's urban core and spreading in all directions, while UHII in Guiyang showed a multi-center agglomeration and emerged in the urban fringes, which also proved that the structure of the urban morphology has a direct influence on the distribution of UHII. Third, the areas of high UHI intensity were dispersed into the suburbs, especially industrial parks and development zones. Kunming's UHI-affected areas occurred with the development of industial parks. In contrast, Guiyang's areas

of high UHI intensity emerged in the development zones, such as Baiyun and Nanming.

4.2 Regression results

The results of multiple linear regression showed that the respective variables were highly significant for the dependent variable (Table 4), and the variance inflation factors (VIF) of all independent variables were less than 10 (Table 5), indicating that there was no serious problem of multicollinearity among the respective variables, but the slightly inferior of goodness of fit were not sufficient to explain the degree of variation in the independent variables, and the results were not of a good explanatory power. Considering the non-stationary spatial variation of temperature, we calculated the local Moran's I index, and the significant Moran's I index indicated the need to consider using spatial econometric models to explore the effects of the respective variables on UHII. The results of LM-Lag and LM-Error significance test show that both spatial lag and spatial error effects are significantly present in the model, indicating the spatial error model and the spatial lag model are applicable.

The analysis of the spatial error model results showed that the PW, EVI, and SLOPE negatively correlated with the urban heat island effect in the karst ecologically fragile area, indicating that specific topographic features may have a mitigating effect on the urban heat island effect; the GSVF had an opposite effect on the heat island effect of the two cities, and showed negative correlation under the influence of mountainous terrain in Guiyang, which may be due to the dispersion of neighborhoods caused by the polycentric urban structure. The BD and PIS of the two cities show a significant positive correlation on the intensity of UHI, which has a significant negative impact on the healthy development of the city. In summary, the different topography and urban form factors of the two cities have a significant effect on the UHI.

The results of random forest regression reveal the extent of the contribution of each independent variable to the urban heat island in the study area (Figure 8). It can be seen that the contribution of each independent variable to the urban heat island intensity in the study areas are overall similar, but there are a little different on USR and SLOPE. USR in Kunming contributes more to the heat island than in Guiyang. SLOPE in Kunming contributes less than in Guiyang. In terms of the degree of contribution of each variable to urban heat island intensity, the EVI was dominant and negative in both monocentric and polycentric urban forms in the karst ecologically fragile zone, which could weaken the UHI; PW was the lowest contributor to the UHII in both cases, but they played an inhibitory role in the UHII; The contribution of SLOPE to urban heat island intensity was different in Kunming and Guiyang, 10.8% and 13.4%, respectively, indicating that mountainous topography inhibits UHII more strongly.

4.3 Influence of topography and urban form factors on UHI

Through the analysis, we found that among the topography factors, in both cites, SLOPE mitigated the urban heat island, while
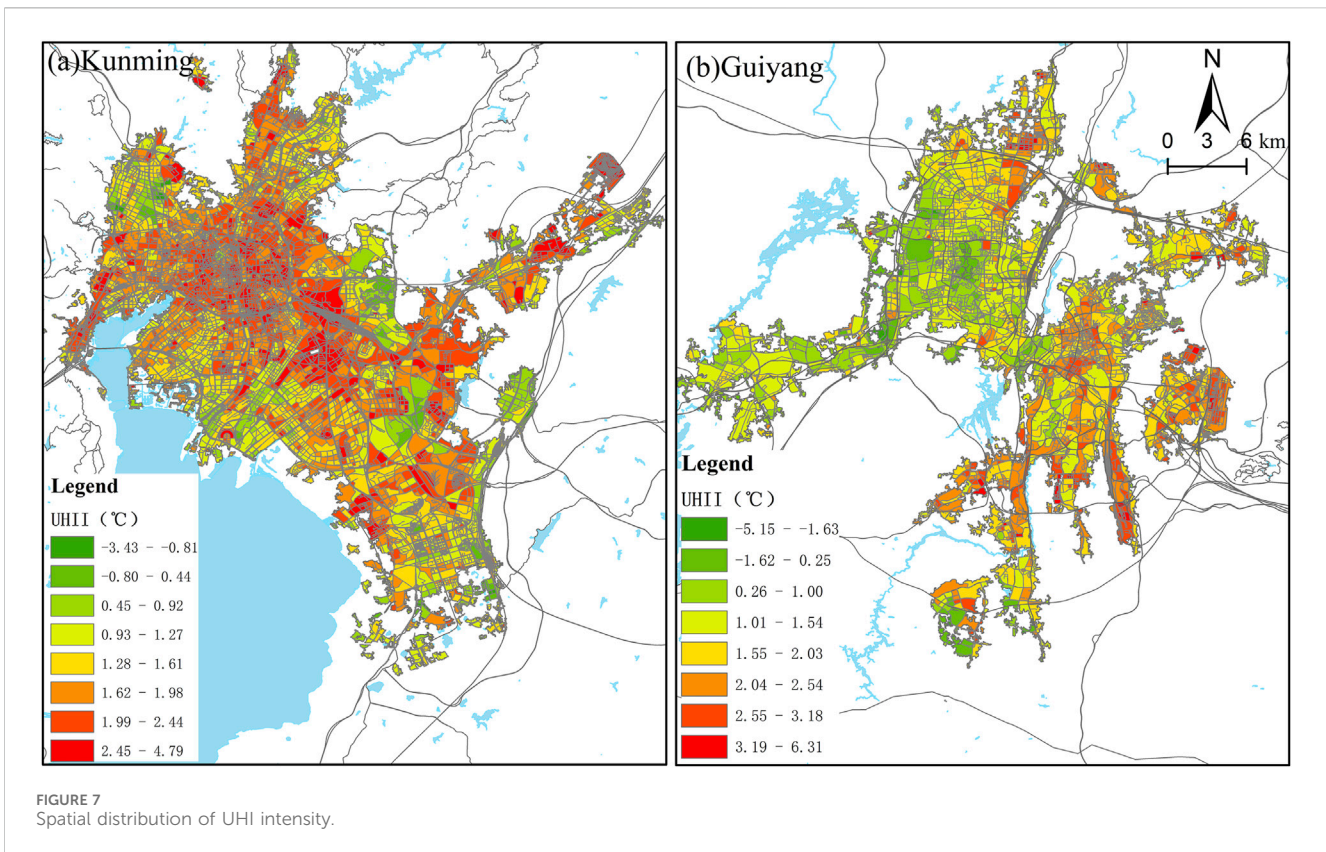
FIGURE 7
Spatial distribution of UHI intensity.

TABLE 3 Descriptive statistics of independent variables.

Variables	Kunming				Guiyang			
	Min	Mean	Max	Standard deviation	Min	Mean	Max	Standard deviation
BD	0.000	0.06	1.000	0.171	0.000	0.04	1.000	3.073
SLOPE	0.000	7.38	154.898	5.891	0.000	12.77	92.758	9.277
PD	0.000	92.28	727.000	114.666	0.000	95.95	1,107	153.094
GSVF	0.152	0.89	1.000	0.198	0.148	0.91	1.000	0.169
USR	0.000	0.85	1.831	0.393	0.000	0.82	1.731	0.417
PIS	0.000	0.85	1.000	0.313	0.000	0.80	1.000	0.431
EVI	0.068	0.24	0.633	0.073	0.000	0.30	0.714	0.083
PW	0.000	0.02	1.218	0.129	0.000	0.01	1.000	0.097

the USR showed positive contribution to UHI. GSVF had opposite impacts on UHI of two cities, showing a negative correlation in Guiyang City, and being positively correlated to the UHI in Kunming, with a similar intensity.

In terms of urban form factors, BD and PD exacerbated the urban heat island, and contributed similarly to the heat island intensity in both cities; The BD and PD of Kunming are concentrated in the main urban areas of Wuhua District, Xishan District, and Guandu District, which are dense and compact, and contribute significantly to the UHI; the multi-center morphology of Guiyang City makes its BD and PD mainly concentrated in the main

urban areas of Nanming, Yunyan, and Guanshanhu Districts, and also in the sub-centers of Wudang and Huaxi, which have a significant contribution to the urban heat island effect to some extent.

Among the land use/cover factors, PIS has the exacerbating effect on UHI. EVI and PW are mitigating factors of UHI, and EVI had the strongest inhibitory effect.

In summary, the monocentric topography of Kunming makes the intensity of urban form factors such as BD, PD, and PIS on UHI especially significant in the central city; Guiyang's complex topography makes the urban form tend to be polycentric in the

TABLE 4 Significance statistics of variables.

Variable	Kunming			Guiyang		
	MLR	SEM	SLM	MLR	SEM	SLM
BD	0.282***	0.199,977***	0.0993,668***	0.399***	0.235,594***	0.134,671***
SLOPE	−0.004***	−0.0050881***	−0.0023090***	−0.014***	−0.0077433***	−0.004031***
PD	0.001***	0.00044694***	0.000136,185***	−5.24e-5*	0.00043778***	2.96769**
GSVF	0.035**	0.00104*	0.0582,322***	0.121***	−0.0297,224**	0.0462,931**
USR	0.169***	0.052506***	0.0434,237***	0.041**	0.0311,837***	0.0268,135***
PIS	0.353***	0.155,049***	0.117,319***	0.324***	0.221,173***	0.149,611***
EVI	−2.472***	−0.936,137***	−0.250,851***	−2.982***	−1.21166***	−0.463,496***
PW	−0.493***	−0.101,617***	−0.101,251***	−0.783***	−0.387,351***	−0.228,048***
λ			0.911,538***			0.88702***
W_{UHI}	34,518	34,518	34,518	20,155	20,155	20,155
n	0.275,018	0.893,559	0.889,018	0.209,987	0.870,410	0.857,971
R^2	−29301.6	−804.168,176	−1,131.51	−201573.1	−60028.7	−6,703.33
LL	58,621.2	16,626.34	2,283.02	43,164.2	12,075.3	13,426.7
AIC	0.282***	0.199,977***	0.0993,668***	0.399***	0.235,594***	0.134,671***
LM-Lag	0.00***			0.00***		
LM-Error	0.00***			0.00***		

Note: LL, means Log likelihood.
AIC, represents Akaike information criterion.
*Significant level $0.05 < p < 0.1$.
**Significant level $0.01 < p < 0.05$.
***Significant level $p < 0.01$.

TABLE 5 Variance inflation factors.

	BD	SLOPE	PD	GSVF	USR	PIS	EVI	PW
Kunming	1.514	1.061	1.767	1.503	1.698	1.434	1.331	1.011
Guiyang	1.373	1.152	1.679	1.501	1.726	1.606	1.196	1.002

process of development, and the more dispersed buildings, roads, and populations help to disperse the heat and reduce the pressure of the urban center's heat island.

5 Discussion

5.1 Impact of topography on UHI

Studies have shown that topographic features significantly affect the spatial distribution of UHI (Mirzaei, 2015; Equere et al., 2021). In karst areas, the complex topography leads to the diversity of urban morphology, which in turn affects the distribution and intensity of UHI. We slected Kunming and Guiyang to compare the UHI in karst region. Kunming has formed a typical single-center city structure with a flat topography about 763 km². With the limitations of nature mountains, Guiyang has been distributed in small and narrow areas. Kunming urban build-up area is concentrated, however Guiyang is dispersive (Figure 2).

Plain terrain areas have a strong UHI effect due to the flat terrain and the centralized distribution of buildings, which leads to the difficulty of heat dissipation. On the contrary, hilly areas have a relatively weak UHI effect due to the undulating topography and the decentralized arrangement of buildings, which is conducive to heat dispersion, as obtained from Figure 7. Areas with larger slopes, with sparse buildings and more green space, help mitigate the heat island effect. However, areas with smaller slopes have higher building density, significant heat accumulation and strong UHI effects. In addition, the appearance of some abnormal heat islands is also related to topographic factors, such as some low-lying areas that lead to significant localized UHI effects due to heat accumulation (Deng et al., 2018; Liao et al., 2022). We also realized that the SLOPE contributed more to mitigate heat island in Guiyang than Kunming. In addition, the Ground Sky View Factor (GSVF) is also an

FIGURE 8
Variable contributions to UHII.
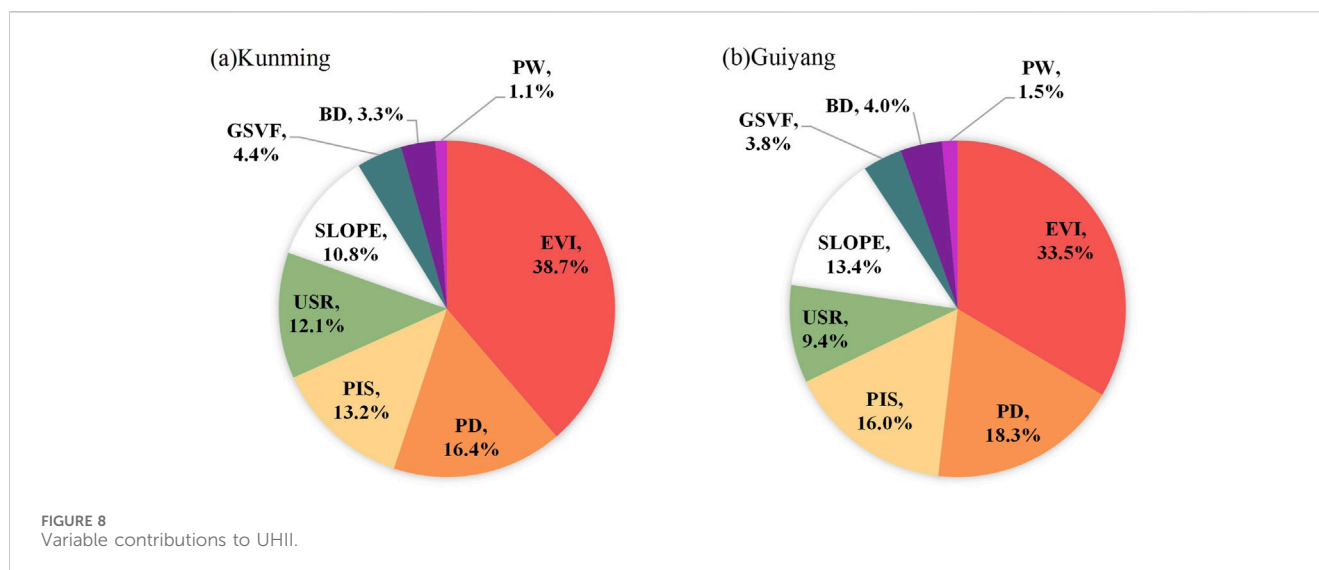
important factor affecting UHI (Liu et al., 2022). A higher GSVF implies an open view between buildings, which may favor the heat dissipation and reduces the UHI effect. On the contrary, a lower GSVF leads to heat accumulation and enhances the UHI effect. The GSVF had an opposite effect on the heat island effect of the two cities (Table 4), and showed negative correlation under the influence of mountainous terrain in Guiyang, which may be due to the dispersion of neighborhoods caused by the polycentric urban structure.

5.2 Impact of urban form on UHI

The effect of urban form on UHI is mainly reflected through building density and population density. We tried to quantify the effects of multiple factors on UHI through spatial econometric modeling and random forest regression modeling, and reveal the contribution of each factor to UHI. In this study, it is found that the UHI effect is significant in high population density areas and high building density areas. This is due to the fact that the concentrated distribution of buildings and population leads to a large amount of artificial heat emission, and it is difficult for heat to dissipate (Figure 8). This study showed that PD contributed more than BD in two cities. The reason may be karst areas are dense population in karst region, Southwest China.

5.3 Impact of land use/cover on UHI

Karst cities have special topography and fragile ecology (Ford and William, 2007), and topography features should be fully considered in planning to rationally layout. The PIS is also an important factor for the magnitude of UHI, with higher PIS increasing surface temperature and exacerbating the UHI effect (Lu et al., 2021). EVI can not only reflect the impact of climate on vegetation but also help predict ecosystem response to climate change (Sun et al., 2021). PW is an important role for the mitigating surface temperature and urban heat island effect (Wang et al., 2015).

The results of random forest regression (Figure 8) revealed the EVI was dominant and negative in both monocentric and polycentric urban forms in the karst ecologically fragile zone. PW also played an inhibitory role in the UHII.

5.4 Practical implications

The findings can offer valuable insights for policymakers and urban planners to optimize the urban form and mitigate the UHI effect in karst area cities. Increasing vegetation area in both single-center and multi-center cities is a good way to mitigate heat island effect. Meanwhile, the mitigation of heat generation can be effectively achieved through the reduction of PIS, PD, and USR. This is particularly important in karst regions where minimizing PD plays a critical role. The heat island intensity of Kunming is evidently associated with the industrial park, thus rationalizing the layout of the industrial park can effectively mitigate the heat island intensity. However, the heat island intensity of Guiyang is closely correlated with the development zone. Therefore, it is advisable to enhance vegetation during the construction phase of the development zone and mitigate impervious water surfaces, reduce population density, and reduce surface roughness. Additionally, this study reveals that SLOPE exerts a significant impact on mitigating the urban heat island effect in karst regions, thus indicating the potential for effectively alleviating urban heat island intensity through strategic utilization of slope to enhance vegetation coverage.

5.5 Research contributions and liminations

In fact, there have been many studies on urban heat island. The contributions of the study as follows:

(1) We paid attention to the UHI in karst region and selected two comparable cities to characterize their UHI. (2) We obtained UHI characteristics of monocentric and polycentric urban form in karst region. (3) We analysed effect of 8 factors on UHI.

That factors, such as topography, urban form, land use/cover, work together to influence the spatial distribution of UHI. Green space and water body have an important moderating effect on the layout of UHI. BD, PIS and URS are positively correlated with the

UHI effect. The contribution of PD is worth to pay more attention in karst region. More works may be conducted for the selection of urban morphology models or spatial indices.

Although this study reveals the effects of topography and urban form on UHI, there are still some shortcomings. Future studies should further deepen the multi-angle and multi-temporal analysis of UHI in karst areas, and explore the changing patterns of UHI in different seasons and under different climatic conditions. In addition, the comprehensive analysis of other influencing factors, such as transportation and energy consumption, should be strengthened. Through scientific and reasonable urban planning, the UHI effect can be effectively mitigated and the sustainable development of the city can be promoted.

6 Conclusion

Comparison of urban heat islands in Kunming and Guiyang reveals the effects of different topography and different urban morphology on the distribution and intensity of urban heat islands in karst regions. The study shows that topography as a natural factor directly affects the urban morphology, thus influencing the distribution and intensity of urban island. The distribution of UHII is higher in single-center cities than in multi-center cities. In single center city Kunming, the areas of high UHII were located in the contiguous urban core and spreaded with development of industial parks, whereas multi-center city Guiyang, the high UHII areas were distributed in several centers related with the development zones. Natural related factors, such as SLOPE, EVI and PW, had similar influences on the mitigation of UHI, and EVI had the strongest mitigating effect. Human related factors, like BD, PD, USR and PIS, exacerbated the UHI, and PD contributed the most to UHI. The above conclusions can provide references for policymakers and urban planners to optimize urban form and mitigate UHI. First, cities can be planned dispersive making use of terrain conditions. Sencond, the area of vegetation and water bodies can be increased. The findings necessitated the implementation of corresponding policy strategies to optimize urban form and enhance the urban thermal environment in karst regions.

Data availability statement

Publicly available datasets were analyzed in this study. This data can be found here: https://earthexplorer.usgs.gov/, https://www.scidb.cn/, https://www.openstreetmap.org/, https://nasadaacs.eos.nasa.gov/, https://www.x-mol.com/groups/li_xuecao/dongtaizhitu.

Author contributions

Funding

Acknowledgments

Conflict of interest

The authors declare that the research was conducted in the absence of any commercial or financial relationships that could be construed as a potential conflict of interest.

Publisher's note

All claims expressed in this article are solely those of the authors and do not necessarily represent those of their affiliated organizations, or those of the publisher, the editors and the reviewers. Any product that may be evaluated in this article, or claim that may be made by its manufacturer, is not guaranteed or endorsed by the publisher.

References

Aboelata, A. (2020). Vegetation in different street orientations of aspect ratio (H/W 1: 1) to mitigate UHI and reduce buildings' energy in arid climate. *Build. Environ.* 172, 106712. doi:10.1016/j.buildenv.2020.106712

Bobb, J. F., Peng, R. D., Bell, M. L., and Dominici, F. (2014). Heat-related mortality and adaptation to heat in the United States. *Environ. health Perspect.* 122 (8), 811–816. doi:10.1289/ehp.1307392

Bokaie, M., Zarkesh, M. K., Arasteh, P. D., and Hosseini, A. (2016). Assessment of urban heat island based on the relationship between land surface temperature and land use/land cover in Tehran. *Sustain. Cities Soc.* 23, 94–104. doi:10.1016/j.scs.2016.03.009

Chen, X., Wang, Z., and Bao, Y. (2021). Cool island effects of urban remnant natural mountains for cooling communities: a case study of Guiyang, China. *Sustain. Cities Soc.* 71, 102983. doi:10.1016/j.scs.2021.102983

Chun, B., and Guldmann, J. M. (2014). Spatial statistical analysis and simulation of the urban heat island in high-density central cities. *Landsc. urban Plan.* 125, 76–88. doi:10.1016/j.landurbplan.2014.01.016

Coseo, P., and Larsen, L. (2014). How factors of land use/land cover, building configuration, and adjacent heat sources and sinks explain Urban Heat Islands in Chicago. *Landsc. Urban Plan.* 125, 117–129. doi:10.1016/j.landurbplan.2014.02.019

Cui, Y., Yan, D., Hong, T., and Ma, J. (2017). Temporal and spatial characteristics of the urban heat island in Beijing and the impact on building design and energy performance. *Energy* 130, 286–297.

Deilami, K., Kamruzzaman, M., and Liu, Y. (2018). Urban heat island effect: a systematic review of spatio-temporal factors, data, methods, and mitigation measures. *Int. J. Appl. earth observation geoinformation* 67, 30–42. doi:10.1016/j.jag.2017.12.009

Deng, Y., Wang, S., Bai, X., Tian, Y., Wu, L., Xiao, J., et al. (2018). Relationship among land surface temperature and LUCC, NDVI in typical karst area. *Sci. Rep.* 8 (1), 641. doi:10.1038/s41598-017-19088-x

Doan, V. Q., Kusaka, H., and Nguyen, T. M. (2019). Roles of past, present, and future land use and anthropogenic heat release changes on urban heat island effects in Hanoi, Vietnam: numerical experiments with a regional climate model. *Sustain. Cities Soc.* 47, 101479. doi:10.1016/j.scs.2019.101479

Equere, V., Mirzaei, P. A., Riffat, S., and Wang, Y. (2021). Integration of topological aspect of city terrains to predict the spatial distribution of urban heat island using GIS and ANN. *Sustain. Cities Soc.* 69, 102825. doi:10.1016/j.scs.2021.102825

Estoque, R. C., Murayama, Y., and Myint, S. W. (2017). Effects of landscape composition and pattern on land surface temperature: an urban heat island study in the megacities of Southeast Asia. *Sci. Total Environ.* 577, 349–359. doi:10.1016/j.scitotenv.2016.10.195

Fahmy, M., and Sharples, S. (2009). On the development of an urban passive thermal comfort system in Cairo, Egypt. *Build. Environ.* 44 (9), 1907–1916. doi:10.1016/j.buildenv.2009.01.010

Fang, C., Wang, S., and Li, G. (2015). Changing urban forms and carbon dioxide emissions in China: a case study of 30 provincial capital cities. *Appl. energy* 158, 519–531. doi:10.1016/j.apenergy.2015.08.095

Ford, D., and Williams, P. D. (2007). *Karst hydrogeology and geomorphology*. John Wiley and Sons.

Grosso, M. (1998). Urban form and renewable energy potential. *Renew. energy* 15 (1-4), 331–336. doi:10.1016/s0960-1481(98)00182-7

Guo, A., Yang, J., Xiao, X., Xia, J., Jin, C., and Li, X. (2020). Influences of urban spatial form on urban heat island effects at the community level in China. *Sustain. cities Soc.* 53, 101972. doi:10.1016/j.scs.2019.101972

Howard, L. (1818). "The climate of London: deduced from meteorological observations, made at different places in the neighbourhood of the metropolis," in *Lombard street, sold also by J. And A. Arch, cornhill; baldwin, cradock, and joy, and W. Bent, Paternoster Row; and J. Hatchard, Picadilly*. Editors W. Phillips and G. Yard.

Jauregui, E. (1997). Heat island development in Mexico City. *Atmos. Environ.* 31 (22), 3821–3831. doi:10.1016/s1352-2310(97)00136-2

Kabano, P., Lindley, S., and Harris, A. (2021). Evidence of urban heat island impacts on the vegetation growing season length in a tropical city. *Landsc. urban Plan.* 206, 103989. doi:10.1016/j.landurbplan.2020.103989

Karunaratne, S., Athukorala, D., Murayama, Y., and Morimoto, T. (2022). Assessing surface urban heat island related to land use/land cover composition and pattern in the temperate mountain Valley City of Kathmandu, Nepal. *Remote Sens.* 14 (16), 4047. doi:10.3390/rs14164047

Kotharkar, R., and Bagade, A. (2018). Evaluating urban heat island in the critical local climate zones of an Indian city. *Landsc. Urban Plan.* 169, 92–104. doi:10.1016/j.landurbplan.2017.08.009

Kotharkar, R., and Surawar, M. (2016). Land use, land cover, and population density impact on the formation of canopy urban heat islands through traverse survey in the Nagpur urban area, India. *J. Urban Plan. Dev.* 142 (1), 04015003. doi:10.1061/(asce)up.1943-5444.0000277

Li, W., Cao, Q., Lang, K., and Wu, J. (2017). Linking potential heat source and sink to urban heat island: heterogeneous effects of landscape pattern on land surface temperature. *Sci. Total Environ.* 586, 457–465. doi:10.1016/j.scitotenv.2017.01.191

Li, X., Zhou, Y., Yu, S., Jia, G., Li, H., and Li, W. (2019). Urban heat island impacts on building energy consumption: a review of approaches and findings. *Energy* 174, 407–419. doi:10.1016/j.energy.2019.02.183

Liang, Z., Wu, S., Wang, Y., Wei, F., Huang, J., Shen, J., et al. (2020). The relationship between urban form and island intensity along the urban development gradients. *Sci. Total Environ.* 708, 135011. doi:10.1016/j.scitotenv.2019.135011

Liao, S., Cai, H., Tian, P., Zhang, B., and Li, Y. (2022). Combined impacts of the abnormal and urban heat island effect in Guiyang, a typical Karst Mountain City in China. *Urban Clim.* 41, 101014. doi:10.1016/j.uclim.2021.101014

Lin, D., Allan, A., and Cui, J. (2013). "Does polycentric urban spatial development lead to less commuting: a perspective of jobs-housing balance," in *49th ISOCARP congress*, 10.

Lin, D., Allan, A., and Cui, J. (2015). The impact of polycentric urban development on commuting behaviour in urban China: evidence from four sub-centres of Beijing. *Habitat Int.* 50, 195–205. doi:10.1016/j.habitatint.2015.08.018

Liu, H., Huang, B., Zhan, Q., Gao, S., Li, R., and Fan, Z. (2021). The influence of urban form on surface urban heat island and its planning implications: evidence from 1288 urban clusters in China. *Sustain. cities Soc.* 71, 102987. doi:10.1016/j.scs.2021.102987

Liu, X., Ming, Y., Liu, Y., Yue, W., and Han, G. (2022). Influences of landform and urban form factors on urban heat island: comparative case study between Chengdu and Chongqing. *Sci. Total Environ.* 820, 153395. doi:10.1016/j.scitotenv.2022.153395

Liu, X., Yue, W., Zhou, Y., Liu, Y., Xiong, C., and Li, Q. (2021). Estimating multi-temporal anthropogenic heat flux based on the top-down method and temporal downscaling methods in Beijing, China. *Resour. Conservation Recycl.* 172, 105682. doi:10.1016/j.resconrec.2021.105682

Lu, Y., Yue, W., Liu, Y., and Huang, Y. (2021). Investigating the spatiotemporal non-stationary relationships between urban spatial form and land surface temperature: a case study of Wuhan, China. *Sustain. Cities Soc.* 72, 103070. doi:10.1016/j.scs.2021.103070

Manoli, G., Fatichi, S., Schläpfer, M., Yu, K., Crowther, T. W., Meili, N., et al. (2019). Magnitude of urban heat islands largely explained by climate and population. *Nature* 573 (7772), 55–60. doi:10.1038/s41586-019-1512-9

Mirzaei, P. A. (2015). Recent challenges in modeling of urban heat island. *Sustain. cities Soc.* 19, 200–206. doi:10.1016/j.scs.2015.04.001

Mo, Y., Bao, Y., Wang, Z., Wei, W., and Chen, X. (2024). Spatial coupling relationship between architectural landscape characteristics and urban heat island in different urban functional zones. *Build. Environ.* 257, 111545. doi:10.1016/j.buildenv.2024.111545

Patz, J. A., Campbell-Lendrum, D., Holloway, T., and Foley, J. A. (2005). Impact of regional climate change on human health. *Nature* 438 (7066), 310–317. doi:10.1038/nature04188

Peng, S., Piao, S., Ciais, P., Friedlingstein, P., Ottle, C., Bréon, F. M., et al. (2012). Surface urban heat island across 419 global big cities. *Environ. Sci. and Technol.* 46 (2), 696–703. doi:10.1021/es2030438

Peng, W., Wang, G., Zhou, J., Zhao, J., and Yang, C. (2015). Studies on the temporal and spatial variations of urban expansion in Chengdu, western China, from 1978 to 2010. *Sustain. Cities Soc.* 17, 141–150. doi:10.1016/j.scs.2015.03.004

Perini, K., and Magliocco, A. (2014). Effects of vegetation, urban density, building height, and atmospheric conditions on local temperatures and thermal comfort. *Urban For. and Urban Green.* 13 (3), 495–506. doi:10.1016/j.ufug.2014.03.003

Ramírez-Aguilar, E. A., and Souza, L. C. L. (2019). Urban form and population density: influences on urban heat island intensities in bogotá, Colombia. *Urban Clim.* 29, 100497. doi:10.1016/j.uclim.2019.100497

Rizwan, A. M., Dennis, L. Y., and Chunho, L. I. U. (2008). A review on the generation, determination and mitigation of Urban Heat Island. *J. Environ. Sci.* 20 (1), 120–128. doi:10.1016/s1001-0742(08)60019-4

Semenzato, P., and Bortolini, L. (2023). Urban heat island mitigation and urban green spaces: testing a model in the city of padova (Italy). *Land* 12 (2), 476. doi:10.3390/land12020476

Stone Jr, B., and Rodgers, M. O. (2001). Urban form and thermal efficiency:*How the Design of cities Influences the urban heat island effect*. *J. Am. Plan. Assoc.* 67 (2), 186–198. doi:10.1080/01944360108976228

Sun, B., Li, W., Zhang, Z., and Zhang, T. (2019b). Is polycentricity a promising tool to reduce regional economic disparities? Evidence from China's prefectural regions. *Landsc. Urban Plan.* 192, 103667. doi:10.1016/j.landurbplan.2019.103667

Sun, G., Jiao, Z., Zhang, A., Li, F., Fu, H., and Li, Z. (2021). Hyperspectral image-based vegetation index (HSVI): a new vegetation index for urban ecological research. *Int. J. Appl. Earth Observation Geoinformation* 103, 102529. doi:10.1016/j.jag.2021.102529

Sun, R., Lü, Y., Yang, X., and Chen, L. (2019a). Understanding the variability of urban heat islands from local background climate and urbanization. *J. Clean. Prod.* 208, 743–752. doi:10.1016/j.jclepro.2018.10.178

Voogt, J. A., and Oke, T. R. (2003). Thermal remote sensing of urban climates. *Remote Sens. Environ.* 86 (3), 370–384. doi:10.1016/s0034-4257(03)00079-8

Wang, S., Baig, M. H. A., Zhang, L., Jiang, H., Ji, Y., Zhao, H., et al. (2015). A simple enhanced water index (EWI) for percent surface water estimation using Landsat data. *IEEE J. Sel. Top. Appl. Earth Observations Remote Sens.* 8 (1), 90–97. doi:10.1109/jstars.2014.2387196

Yan, J., Yin, C., An, Z., Mu, B., Wen, Q., Li, Y., et al. (2023). The influence of urban form on land surface temperature: a comprehensive investigation from 2D urban land use and 3D buildings. *Land* 12 (9), 1802. doi:10.3390/land12091802

Yue, W., Qiu, S., Xu, H., Xu, L., and Zhang, L. (2019). Polycentric urban development and urban thermal environment: a case of Hangzhou, China. *Landsc. urban Plan.* 189, 58–70. doi:10.1016/j.landurbplan.2019.04.008

Zhang, T., Sun, B., and Li, W. (2017). The economic performance of urban structure: from the perspective of Polycentricity and Monocentricity. *Cities* 68, 18–24. doi:10.1016/j.cities.2017.05.002

Zhao, L., Lee, X., Smith, R. B., and Oleson, K. (2014). Strong contributions of local background climate to urban heat islands. *Nature* 511 (7508), 216–219. doi:10.1038/nature13462

Zhou, B., Rybski, D., and Kropp, J. P. (2017). The role of city size and urban form in the surface urban heat island. *Sci. Rep.* 7 (1), 4791. doi:10.1038/s41598-017-04242-2

Zhou, D., Xiao, J., Bonafoni, S., Berger, C., Deilami, K., Zhou, Y., et al. (2018). Satellite remote sensing of surface urban heat islands: progress, challenges, and perspectives. *Remote Sens.* 11 (1), 48. doi:10.3390/rs11010048

Zhou, D., Zhao, S., Liu, S., Zhang, L., and Zhu, C. (2014). Surface urban heat island in China's 32 major cities: spatial patterns and drivers. *Remote Sens. Environ.* 152, 51–61. doi:10.1016/j.rse.2014.05.017

Zhou, W., Huang, G., and Cadenasso, M. L. (2011). Does spatial configuration matter? Understanding the effects of land cover pattern on land surface temperature in urban landscapes. *Landsc. urban Plan.* 102 (1), 54–63. doi:10.1016/j.landurbplan.2011.03.009

Zhou, X., and Chen, H. (2018). Impact of urbanization-related land use land cover changes and urban morphology changes on the urban heat island phenomenon. *Sci. Total Environ.* 635, 1467–1476. doi:10.1016/j.scitotenv.2018.04.091